POLITECNICO DI TORINO
Repository ISTITUZIONALE

Joining mechanisms and mechanical properties of PA composites obtained by selective laser sintering

(Article begins on next page)

28 April 2024

Joining mechanisms and mechanical properties of PA composites obtained by selective laser sintering

Elena Bassoli and Andrea Gatto

Department of Mechanical and Civil Engineering, University of Modena and Reggio Emilia, Modena, Italy, and

Luca Iuliano

Department of Manufacturing Systems and Economics, Politecnico di Torino, Torino, Italy

Abstract

Purpose – Additive manufacturing is today a viable industrial solution alongside traditional processes. Techniques like selective laser sintering (SLS) address the issues of digital production and mass customization in a variety of materials. Composite parts can be obtained with specific functional and mechanical properties. Building orientation during additive manufacturing often causes anisotropy of parts' properties that is still unspecified in technical information. The purpose of this paper is to investigate the mechanical performances and failure mechanisms of an aluminium-filled polyamide and of a new alumina-polyamide composite produced by SLS, in comparison with unfilled PA.

Design/methodology/approach – A specific focus is set on the evaluation of primary and secondary anisotropy in the case of metal or ceramic filler, as well as on the specific contribution of powder distribution modes and joining phenomena. Macroscopic mechanical tests and the observation of joining and failure micro-mechanisms are integrated.

Findings – The results prove the absence of relevant anisotropy amongst specimens that are produced with the axis parallel to the plane of powder deposition. Samples whose axis is parallel to the growth direction Z, instead, reveal a significantly different response with respect to other orientations.

Originality/value – An original explanatory model is assumed and validated, based on an anisotropic distribution of the reinforcing particles during parts' production, which determines the efficacy of the strengthening mechanisms during crack propagation.

Keywords Polyamides, Sintering, Composite materials, Additive manufacturing, Selective laser sintering, Aluminium, Alumina

1. Introduction

Layer manufacturing technologies originated as a novel prototyping capability but are turning today into industrial solutions for regular production beside traditional processes (Bernard *et al.*, 2009). The prototyping function is just one, and no more the most crucial, of their many possible uses (Wohlers, 2009). International standards recently validated a new categorization, replacing the concepts of rapid prototyping and manufacturing with the definition of additive manufacturing (AM) as "a process of joining materials to make objects from 3D model data, usually layer upon layer, as opposed to subtractive manufacturing methodologies" (ASTM F2792-09, 2009).

Layer manufacturing allows rapid product development and production, ensures shortening the time to market and developing customized production with affordable costs (Bernard *et al.*, 2009). In addition, additive fabrication opens new manufacturing frontiers, enabling geometries and structures impossible to be obtained by traditional processes.

Freedom to design complex geometries results in a new approach to industrial product design: improved or novel functionalities can be achieved and several parts of an assembly be integrated in a single sophisticated item (Atzeni *et al.*, 2012). Ease of obtaining geometrical complexity is also leading to many applications of AM in the medical field. Layer fabrication is already applied to the production of customized dental, maxillofacial and orthopedic prostheses (Atzeni *et al.*, 2009; Vandenbroucke and Kruth, 2007; Bibb *et al.*, 2010). Moreover, many researchers are studying layer production of scaffolds for cell growth, whose potential effects could be impressive (Toni *et al.*, 2009; Giannatsis and Dedoussis, 2009). Besides geometry, complexity can be attained through AM also in microstructure or composition. A strong attention is currently driven by the chance of layer manufacturing controlled variations of material composition within a product, moving towards functionally-graded materials (FGM). To this aim, the inherent unhomogeneity of AM should be exploited to tune parts' properties (Bernard *et al.*, 2009; Caulfield *et al.*, 2007). Industrial spin-offs related to the full exploitation of AM technologies would be strategic (Wohlers, 2009).

The AM technique that best fits direct digital production and mass customization is selective laser sintering (SLS).

It offers high throughput, no need for supports except from the first layers to be detached from the machine worktable, no post-processing, wide range of materials, high automation possibilities (Eyers and Dotchev, 2010; Bassoli *et al.*, 2005; Caulfield *et al.*, 2007). Fully functional components can be obtained for example in polyamide (unfilled or reinforced with glass fibres/beads, Aluminium and carbon), flame retardant polyamides and Polyetheretherketone (PEEK) for automotive, aerospace and military industries, but also biomedical devices and consumer goods (Eyers and Dotchev, 2010; Berti *et al.*, 2010; Senthilkumaran *et al.*, 2009). Polyamide-matrix composite parts can be produced directly from the CAD model, without any post-treatment.

Aluminium-reinforced polyamide produced by SLS combines short times and low costs with much higher stiffness than plain PA and capability to withstand relatively high temperatures. Moreover, the full density of laser-sintered parts ensures an excellent surface finish after grinding or polishing (Violante *et al.*, 2007). Interesting applications regard functional prototypes, even for critical tests such as in the wind tunnel for automotive applications, metallic-painted illustrative models or end products for specific applications (Violante *et al.*, 2007). Besides, Aluminium-filled polyamide is marketed for Rapid Tooling applications, following the trend to use metal-polymer composites for the production of mould inserts for small pre-series (Masood and Song, 2004; Yang and Ryu, 2001).

A formulation of Alumina-filled polyamide, still unavailable on the market, has been studied to obtain high stiffness and strength retained up to 100°C (Berti *et al.*, 2010). The results pointed out an anisotropic response of parts. In first instance, a primary anisotropy is present that differs the growth direction from any direction in the plane of powder deposition. Parts' properties along the *Z*-direction are mainly influenced by the junction between different layers. In addition, a secondary less relevant anisotropy can be noticed between different directions parallel to the XY plane, due to the kinematics of powder deposition and to laser tool path. Close to the upper limit of the temperature range, parts produced along the two main directions within the XY plane show different responses. The above consideration is in good accordance with previous researches on various AM technologies, which lead to introduce the concepts of primary and secondary anisotropy. Primary anisotropy is relative to the growth direction and is due to layer construction, secondary anisotropy is introduced in some AM processes by inherent anisotropic mechanisms of material deposition or heat supply (Bassoli *et al.*, 2009; Berti *et al.*, 2010). Metal and ceramic fillers could show differences in powder's distribution within each layer. Many studies concerning SLS parts confirm the importance of fabrication parameters and geometry on the final performances, due to anisotropic heat supply and transfer phenomena that cause the powder melting and consolidation (Kruth *et al.*, 2003; Gibson and Shi, 1997; Bugeda *et al.*, 1999). On the other hand, the increasing interest in virtual prototyping lead to the development of numerical models for the SLS process that still do not take into account anisotropic effects between the powder deposition plane and the growth direction *Z* (Bugeda *et al.*, 1999). For this reason, they are not totally efficient yet in describing the parts' performances. Other analytical models for temperature distribution suggest the relevance of the volume fraction of gases in the powder bed

(Zhang and Faghri, 1999). Thus, the anisotropy introduced with powder deposition would turn into anisotropic thermal conductivity and energy absorption (Williams and Deckard, 1998; Zhu *et al.*, 2007; Kruth *et al.*, 2003; Bugeda *et al.*, 1999; Zhang and Faghri, 1999).

Despite the above considerations, technical specifications are still undifferentiated for the various directions within the AM system and little is known as to the variations in the mechanical response. The need for predictability and repeatability of the mechanical characteristics is stated by many researchers as the basis for the industrial acceptance of AM processes (Gibson and Shi, 1997; Berti *et al.*, 2010; Caulfield *et al.*, 2007; Senthilkumaran *et al.*, 2009). The present research aims at studying tensile behavior and hardness of a polyamide and two polyamide-matrix composites produced by SLS, evaluating the presence of primary and secondary anisotropy and mapping the mechanical response as a function of the building geometry. The latter is a key aspect for the successful design and industrial exploitation of parts built by AM. To this regard, it is important to evidence that the study deals with materials that are commercially available: the objective is not to develop new formulations, but to contribute to standardization and knowledge on the industrial material-process combinations. Moreover, the research addresses the investigation of joining mechanisms that occur during AM of the considered materials, their relation to the mechanical properties and failure modes and their effect on anisotropy.

2. Materials and methods

Tests are conducted on specimens produced by SLS with three materials:
1 unfilled Polyamide 12 (PA 2200®), named PA in the following;
2 Alumium-filled Polyamide 12 (Alumide®), named PA + Al; and
3 Alumina-filled Polyamide 12 (new on the market, provided as a beta-test), marked as PA + Al_2O_3.

Datasheets are available for two of the above materials: Table I lists tensile strength at break (σ_u), strain at break (ε_u), modulus of elasticity (E), Shore hardness and density of the laser-sintered parts. It should be noticed that nominal data are undifferentiated as to the building orientation.

Cylindrical tensile specimens are produced on a SLS machine, following the specifications of ASTM D638-08 (2008): diameter and length of narrow section are 6 and 65 mm, respectively. Standard process parameters of the SLS system for the considered materials are adopted.

Specimens are built in different orientations as to the distinctive directions within the SLS machine,

Table I Mechanical properties reported in the data sheet, for parts obtained by SLS with standard parameters

		PA 2200®	ALUMIDE®
E	MPa	1,700	3,600
σ_u	MPa	45	45
ε_u	%	20	3
Shore hardness		75 (shore A)	76 (shore D)
Density	g/cm³	0.9-0.95	1.37-1.43

chosen to address the issues of primary and secondary anisotropy. The manufacturing geometry is shown in Figure 1, where the plane of powder deposition is named XY and the growth direction Z: specimens are built in X, Y, XY and Z directions. The axis of X and Y specimens coincide, respectively, with the powder re-coater speed vector and its perpendicular direction; XY samples lay on the bisector of the X and Y directions; the axis of Z specimens is parallel to the growth direction.

Thermogravimetric analysis (TGA) is carried out on the materials to study the weight percentage of Aluminium and Alumina as reinforcements. The test is conducted on 20 mg samples from room temperature to 1,273 K with a heating rate of 40 K/min, in air (Perkin-Elmer TGA7). Porosity is measured through image binarization and analysis on polished sections of the sintered specimens (five measurements for each material). For comparison, Archimedes density is also determined on the two filled materials (six measurements each).

Ultimate tensile strength (UTS) tests are carried out using self-centering equipment. Strain is measured using an extensometer on a gage length of 25 mm. A testing speed of 2.5 mm/min is adopted, which ensures values of strain rate inferior to $0.008 \, s^{-1}$ (ASTM D638-08, 2008). A load cell with a capacity of 5 kN is employed. Five specimens are tested for each combination of material and orientation.

Shore D hardness (SHD) is measured on surfaces orthogonal to the samples' axis, which means for example that the results for X specimens refer to the ZY surface and that on the whole hardness is tested in all the relevant orientations. Shore A preliminary tests on PA parts provided values near to the scale maximum.

Statistical tools are applied to the evaluation of the results: in particular the t-test for independent samples is used to identify the existence of significant differences between the groups of specimens, that is to confirm primary or secondary anisotropy. The p-level reported with a t-test represents the probability of error involved in rejecting the null hypothesis, i.e. accepting the existence of a difference between two groups of specimens. A level of significance of 0.01 is chosen.

Rupture surfaces after the tensile tests, as well as the un-sintered powder, are observed using the scanning electron microscope (SEM) in order to investigate failure mechanisms and joining phenomena between the particles. Both secondary and back-scattered electrons are used, with the aid of semi-quantitative EDS microanalysis.

3. Results and discussion

3.1 Thermo-gravimetric analysis and density measurements

TG curves in Figure 2 show that the PA matrix decays at 730 K with a weight loss of 100 per cent. The Aluminium-filled composite at the same temperature looses 48 per cent of the total mass. The Alumina-filled PA undergoes a weight loss in two consecutive steps, starting around 480 K and finishing around 750 K, with an overall mass loss of 55 per cent. The analysis assesses the weight percentage of fillers in the two composite materials at 52 per cent for Aluminium and 45 per cent for Alumina. The nominal density of $PA + Al_2O_3$ can thus be calculated at 1.38-1.45 g/cm^3.

Polished sections show that unfilled PA is 100 per cent dense and few pores can be detected in the two composites. Percentage porosity calculated by image analysis is 0.44 per cent (SD = 0.15 per cent) for PA + Al and 0.38 per cent (SD = 0.10 per cent) for $PA + Al_2O_3$. The results are confirmed by Archimedes density, that is 1.41 g/cm^3 for the Al-filled material and 1.44 g/cm^3 for the Alumina-filled one. Both values amount to 99.6 per cent of the nominal density.

3.2 UTS and hardness tests

The results of UTS and hardness tests are shown in Table II, separately for the different directions. Figure 3 shows the stress-strain curves of representative specimens, whose strength and strain at break are the nearest to the mean values of each group. The same scale is adopted for the three graphs, to allow direct comparison. The Aluminium-filled parts of X, Y and XY groups show a maximum in the σ-ε curve. Standards specific for polymeric materials (ASTM D638-08, 2008) define the point of zero slope of the stress-strain curve as the yield point, where the value of stress is the tensile strength at yield (σ_y). This definition differs from standard conventions referring to an offset yield, but matches the peculiar response of polymeric materials (Dasari and Misra, 2003). For these specimens σ_y is indicated in addition to stress and strain at break (σ_u, ε_u). For the same material, no zero-slope point can be observed for specimens produced in the Z-direction. Unreinforced and Alumina-filled polyamide do not show a zero-slope yield point either, so tensile strength and strain at break are calculated (σ_u, ε_u).

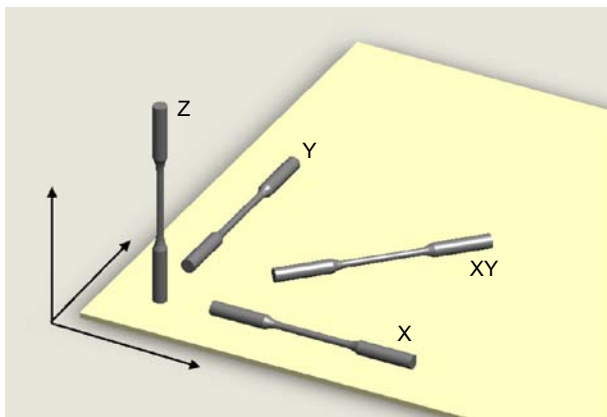**Figure 1** Specimens construction geometry

Figure 2 TG curves
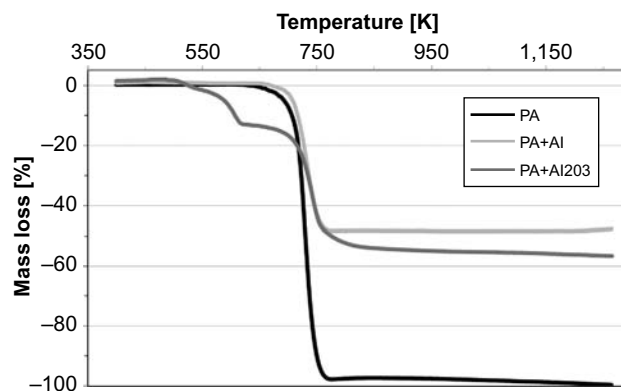
Table II Results for elastic modulus (E), tensile strength at yield σ_y, tensile strength at break σ_u, strain at break ε_U (ASTM D638-00) and shore hardness (SHD)

		E (MPa) Mean (SD)	σ_y (MPa) Mean (SD)	σ_u (MPa) Mean (SD)	ε_u (%) Mean (SD)	SHD Mean (SD)
PA	X	1,270 (45.7)		33.6 (0.23)	12 (0.93)	68 (1.2)
	Y	1,300 (15.0)		33.7 (0.31)	11 (0.70)	70 (1.8)
	XY	1,350 (78.9)		35.7 (1.55)	13 (1.22)	67 (1.8)
	Z	1,420 (160)		44.5 (0.44)	11 (0.35)	74 (0.8)
PA + Al	X	2,960 (55.0)	35 (0.8)		3.6 (0.28)	75 (2.5)
	Y	2,920 (85.4)	34 (0.5)		3.3 (0.36)	78 (1.0)
	XY	3,080 (45.3)	34 (1.0)		2.9 (0.29)	77 (1.0)
	Z	2,730 (230)		32 (0.8)	1.9 (0.12)	76 (0.6)
PA + Al$_2$O$_3$	X	4,170 (240)		24.1 (3.50)	1.6 (0.27)	74 (1.9)
	Y	3,950 (490)		22.9 (1.15)	1.6 (0.50)	74 (2.0)
	XY	3,870 (450)		24.3 (0.83)	1.5 (0.44)	73 (0.8)
	Z	3,460 (306)		17.7 (1.16)	0.8 (0.12)	76 (1.6)

Figure 3 Stress-strain curves
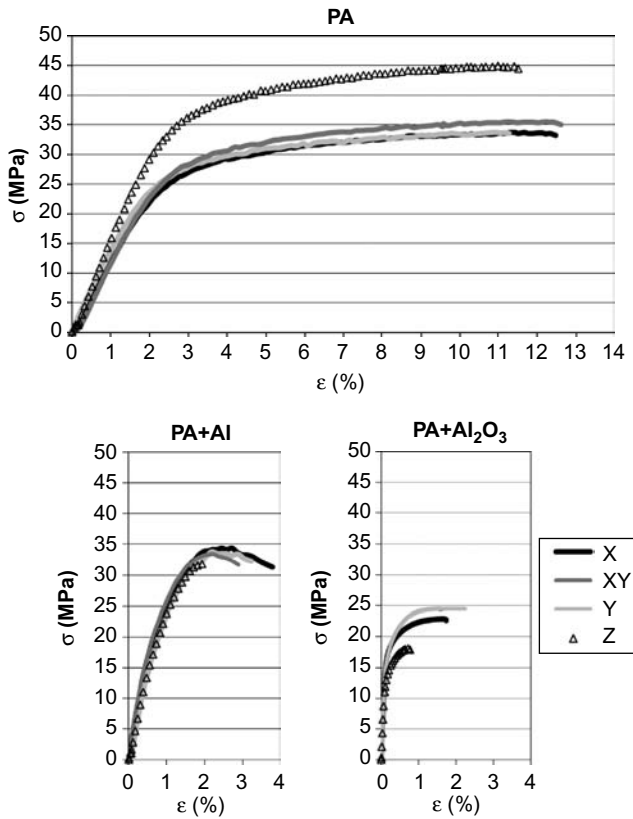
The modulus of elasticity (E) is also worked out as the slope of the tangent to the stress-strain curve within the proportional limit. Despite the debate on the existance of a true proportional limit for polymeric materials, the value of E has to be regarded as a useful engineering parameter. Standard deviations (SD), listed between brackets beside mean values, attest very high consistency of all measurements.

Strength of PA parts (33-35 MPa) is approximately 30 per cent lower than the nominal value, except for Z specimens that are definitely stronger than all other groups (45 MPa). Strain at break is only about half the value in the datasheet (11-13 per cent). As to Aluminium-filled PA, strain at break is very close to the nominal value (around 3 per cent) except for Z parts, but strength is 30 per cent lower than in the datasheet (35 MPa). A fairly good accordance with technical specifications can be observed as to the elastic modulus for PA and PA + Al, in the range 1,300-1,400 and 2,700-3,100 MPa, respectively. Elastic modulus of the Alumina-filled material is around 4 GPa. Shore hardness of PA specimens is higher than stated in the datasheet (68-74SHD). For the two composites SHD readings are very similar, close to the nominal value for PA + Al (74-77SHD) and only slightly higher than the unreinforced material. This can be ascribed to a mechanism of surface resistance to indentation that relies on a lower plastic flow capability of the PA matrix due to the reinforcing particles, independent on the filler's mechanical properties. If instead the composite hardness was determined by a blending rule between the two components, PA + Al$_2$O$_3$ would have been much harder than the Aluminium-filled material.

A comparison between tensile results of the three materials shows that fillers cause no increase or even a decay in strength that, at least for PA + Al, is not contemplated in the datasheet, but they are effective in increasing parts' stiffness. The reinforcing particles also lead to a strong reduction in strain at break with respect to PA, to a higher extent for Alumina. Focusing on the different manufacturing directions, the results do not point out evident differences amongst X, Y and XY specimens. In Z-direction a lower strain at break can be remarked for PA + Al and PA + Al$_2$O$_3$ parts, approximately half the value in the other directions. Aluminium-filled Z parts fail before the yield point, but reach strength values comparable with the other directions. Alumina-filled Z specimens, instead, are about 30 per cent weaker than the ones parallel to the XY plane. On the contrary unfilled PA specimens in the Z-direction show the highest values of strength, which is quite rare in the field of AM technologies.

Anisotropy in the mechanical response is first assessed through statistical tools, then the understanding of the mechanism of anisotropy is deepened through the observation of failure mechanisms in the last section of the results. The t-test for independent groups is carried out, comparing for each material the different manufacturing orientations. For PA + Al specimens the test is conducted on the value of strength, either at yield or break (σ_y/σ_u), whichever is relevant for the considered direction, the same as listed in Table II. This approach relies on the choice to consider the maximum stress in the σ-ε curve as the most relevant parameter for parts' response. The results are shown in Table III that reports the p-values for the variables σ_y/σ_u, ε_u and SHD analyzed between the groups X, Y, XY and Z for the three materials. Significant differences are obtained for nearly all the comparisons between Z and the other directions, whereas p-values are higher than the adopted level of significance amongst specimens produced in the XY plane. In particular, unfilled PA in the growth direction Z shows significant differences compared to X, Y and XY specimens only as regards strength and hardness, whereas for the filled materials the t-test is positive for all comparisons with Z group for strength and strain at break. The disparities between hardness values are less sharp than for the other variables. This can be due to the described mechanism ruling the resistance to indentation.

4

Table III *p*-values resulting from the *t*-test for the variables σ_y/σ_u, ε_u and SHD among the groups X, Y, XY and Z

		X vs Y	X vs XY	Y vs XY	X vs Z	Y vs Z	XY vs Z
PA	σ_u	0.493	0.058	0.040	*< 0.01*	*<0.01*	*< 0.01*
	ε_u	*< 0.01*	0.653	0.017	*<0.01*	0.411	0.056
	SHD	0.092	0.166	0.019	*<0.01*	*<0.01*	*<0.01*
PA+Al	σ_y/σ_u	0.195	0.207	0.694	*0.01*	*0.01*	*0.01*
	ε_u	0.475	0.037	0.131	*< 0.01*	*<0.01*	*<0.01*
	SHD	0.095	0.351	0.187	0.798	*0.01*	0.134
PA+Al$_2$O$_3$	σ_u	0.466	0.924	0.058	*< 0.01*	*<0.01*	*<0.01*
	ε_u	0.988	0.531	0.679	*< 0.01*	*<0.01*	*0.01*
	SHD	0.938	0.408	0.389	0.162	0.206	0.015

Note: Values below the level of significance of 0.01 are italicised

The 8 observations in the above paragraph are thus confirmed by the statistical analysis. For the considered materials and manufacturing strategy the presence of primary and the absence of secondary anisotropy is demonstrated.

3.3 Failure mechanisms observation

PA specimens show homogeneous rupture surfaces, with some disparities between Z and the other directions. Figure 4 exemplifies the morphology observed for X, Y and XY specimens (Figure 4(a)) and Z specimens (Figure 4(b)). In Figure 4(a) the slices typical of layer manufacturing can be observed on X parts, but the connection between over and under layers is high enough to that failure for loads parallel to the growth direction (i.e. for Z parts) occurs within and not in-between layers (Figure 4(b)). Instead, the disparity in the numerical values of specimens' strength corresponds to a higher presence of voids on the rupture surface of X, Y and XY parts with respect to Z parts, which could be ascribed to insufficient overlap of laser paths on the XY plane.

As to the reinforced materials, two distinct areas with different failure morphologies can be detected on the rupture surfaces of all the specimens, with some differentiations analyzed in the following. Referring to the scheme in Figure 5, a first area (Figure 5(a)) presents numerous reinforcing particles emerging from the polyamide matrix, which shows high plastic strain. In the remaining region (Figure 5(b)) filler particles are submerged in the matrix and failure mechanisms appear considerably different, without signs of strain. Specimens' failure occurs in

two distinct moments with different modalities. Previous studies specifically investigated this aspect through observations after interrupted tests and proved that cracks originate from the external surface and propagate initially with the B morphology to end with ductile strain of the polymeric matrix in the remaining section (Berti *et al.*, 2010).

The examination of rupture surfaces allowed assuming a model for the consolidation phenomena, which is capable to account both for the observed failure mechanisms and the anisotropy in the mechanical performances. Un-sintered powder of the two filled materials is shown in Figure 6, where the shape of reinforcing particles can be appreciated: Aluminium particles are ellipsoids, Alumina ones are polyhedral aggregates. During the deposition of each layer in the AM machine, filler particles are laid with the main axis in the XY plane. Laser treatment causes the polymer to melt, reducing its viscosity. Since, the density of Aluminium and Alumina is more than double with respect to polyamide, the reinforcements partially sink in the matrix and a bedding phenomenon in obtained in the Z-direction. The result is the presence of layers parallel to the XY plane with a lower volume fraction of reinforcement, evidenced in the scheme in Figure 7(a) by the thick gray lines. Figure 7(b) and (c) show examples of the many clusters of reinforcing particles stacked on XY planes that can be observed on polished sections of the specimens.

This anisotropy in the orientation and distribution of fillers determines the efficacy of the strengthening mechanisms during crack propagation. In effect, at a higher level of detail, a distinction can be made between the rupture surfaces of specimens with the axis laying on the plane of powder deposition, on the one side, and Z specimens on the other. For X, Y and XY specimens the area of ductile failure A is wide and reinforcing particles emerge from the matrix also in the B zone. A transition zone C can be observed, where the failure mechanisms change from one mode to the other. Figure 8 shows examples of the described areas for an Aluminium-filled specimen. The observed morphology can be justified considering that the particles' distribution assumed for these samples is effective in obstructing crack propagation, through the reinforcing mechanisms of crack deviation and deflection, as schematized in Figure 9(a). For this reason the ductile failure mode involves a large area fraction and the samples show a zero-slope yield point.

For specimens with the axis parallel to the Z-direction, instead, the area of ductile morphology A is considerably

Figure 4 Rupture surface of PA parts:

(a)	(b)
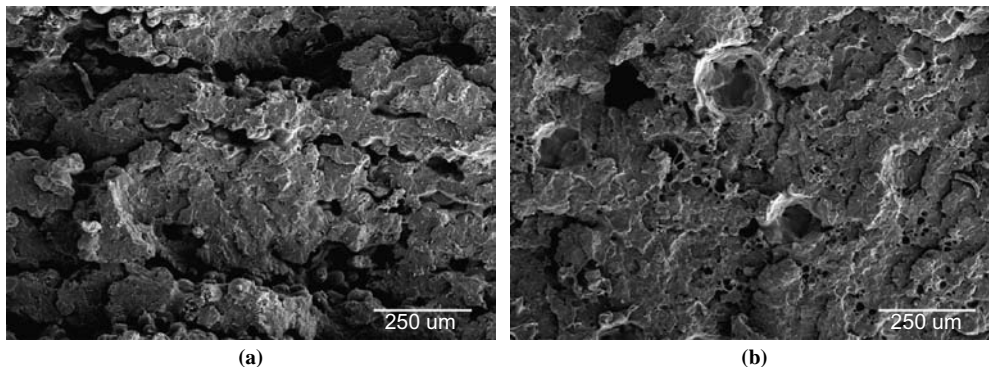
Notes: (a) X specimen; (b) Z specimen

Figure 5 Two different areas on the rupture surface of PA + Al and PA + Al$_2$O$_3$ specimens
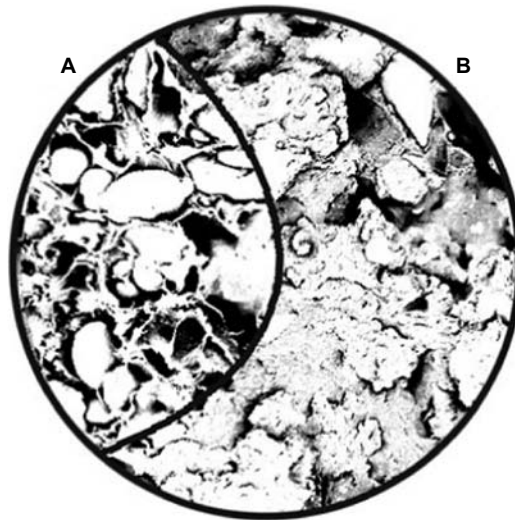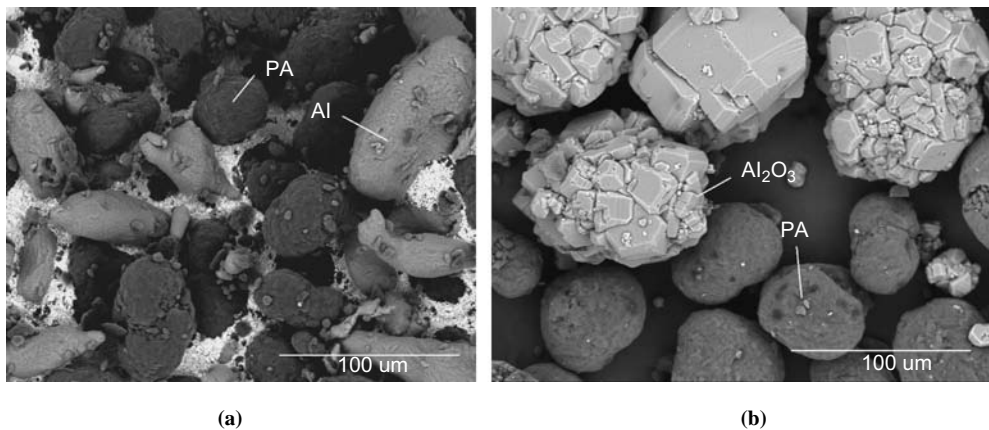

Figure 6 Unsintered PA + Al (a) and PA + Al$_2$O$_3$ (b) powder

(a)

(b)

smaller and filler particles do not emerge from the matrix in the B zone. Figure 10 exemplifies the described phenomenon for the Aluminium-filled composite. Even at a higher magnification, the metal particles are clearly submerged and failure occurs in the polymeric matrix. Due to particles' anisotropic orientation and distribution, for loads applied in the Z-direction the reinforcement is less effective and failure propagates through the layers characterised by low volume fraction of filler (Figure 9(b)). The described mechanisms account for the limited area interested by a ductile failure mode and for the absence of a zero-slope yield point in the σ-ε curves.

The same can be observed on Alumina-filled parts (Berti *et al.*, 2010).

Conclusions

In this research, the mechanical performances and failure mechanisms of Aluminium-filled polyamide and of a "beta-test" Alumina-polyamide composite produced by SLS are studied and compared with unfilled PA. The experimental plan provides a specific focus on the evaluation of primary and secondary anisotropy, introduced both by powder deposition and laser sintering.

Shore hardness is not significantly increased by the reinforcement, proving that resistance to surface indentation does not follow a blending rule. Elastic modulus is considerably higher for the filled materials than for plain PA. Fillers do not guarantee any increase, or in some cases determine a decay, in parts' strength.

As regards anisotropy mechanical results, analysed through statistical tools, and failure mechanisms observation prove that no relevant anisotropy can be noticed amongst specimens produced with the axis parallel to the plane of powder deposition. This is true for all the material formulations. Thus, laser toolpath and process parameters are effective in ensuring isotropic characteristics within the XY plane. Samples with the axis parallel to the growth direction Z, instead, reveal a significantly different response with respect to the other orientations. In particular, unfilled PA Z specimens are stronger than the other directions, whereas the two composites show in the Z-direction lower strength and, to a greater extent, lower strain at break.

Based on the observation of rupture surfaces and on their correlation to the mechanical tests, an original explanatory model is assumed, based on an anisotropic distribution of the reinforcing particles during parts' production, which

6

Figure 7 Bedded structure originated during laser sintering

x, y
(a)

z

x
(b)   (c)
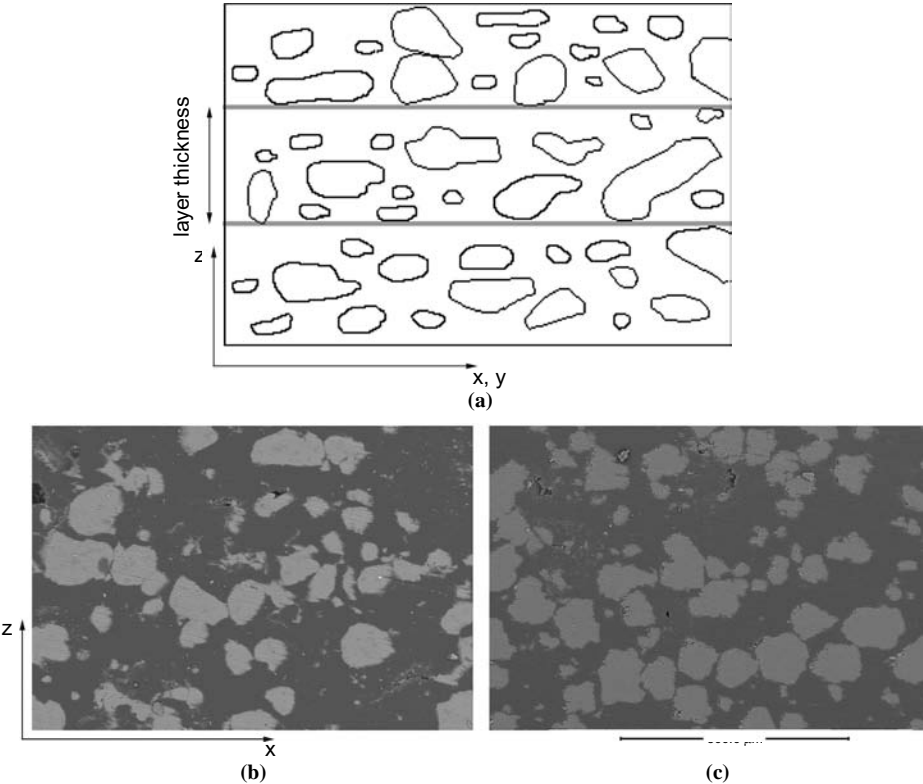
Notes: (a) Scheme; ((b) and (c)) polished sections of a PA + Al (b) and of a PA + Al_2O_3 (c) part

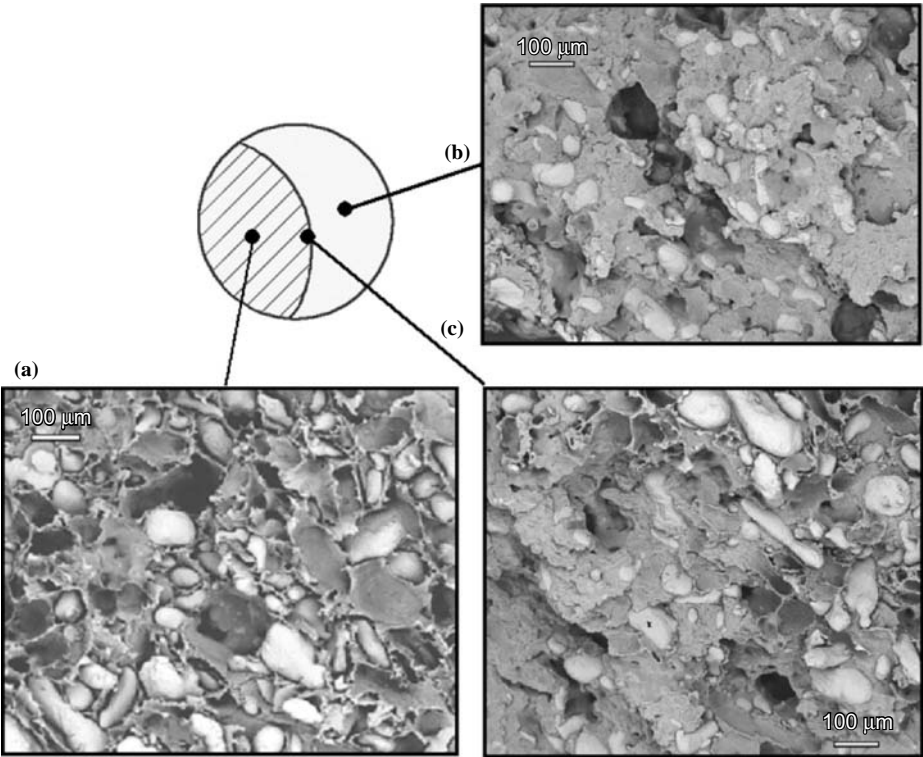**Figure 8** Rupture surface typical of PA + Al specimens with the axis // to X, Y and XY directions

(b)

100 μm

(c)

(a)

100 μm

100 μm

Figure 9 Failure mechanisms for specimens with the axis // to: (a) X, Y, and XY directions; (b) Z direction
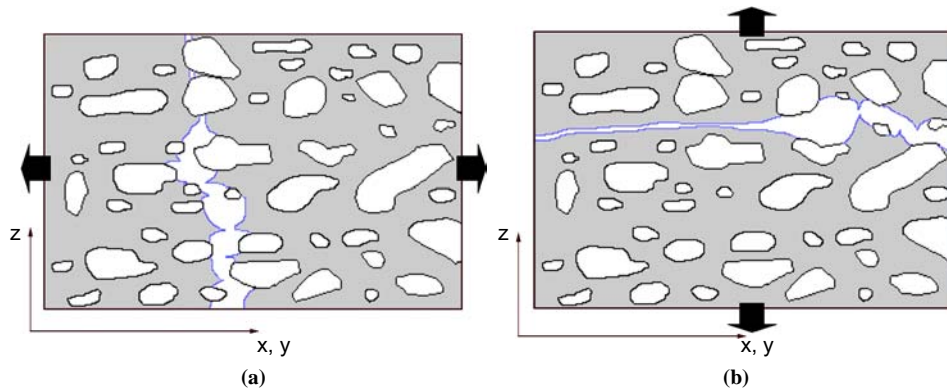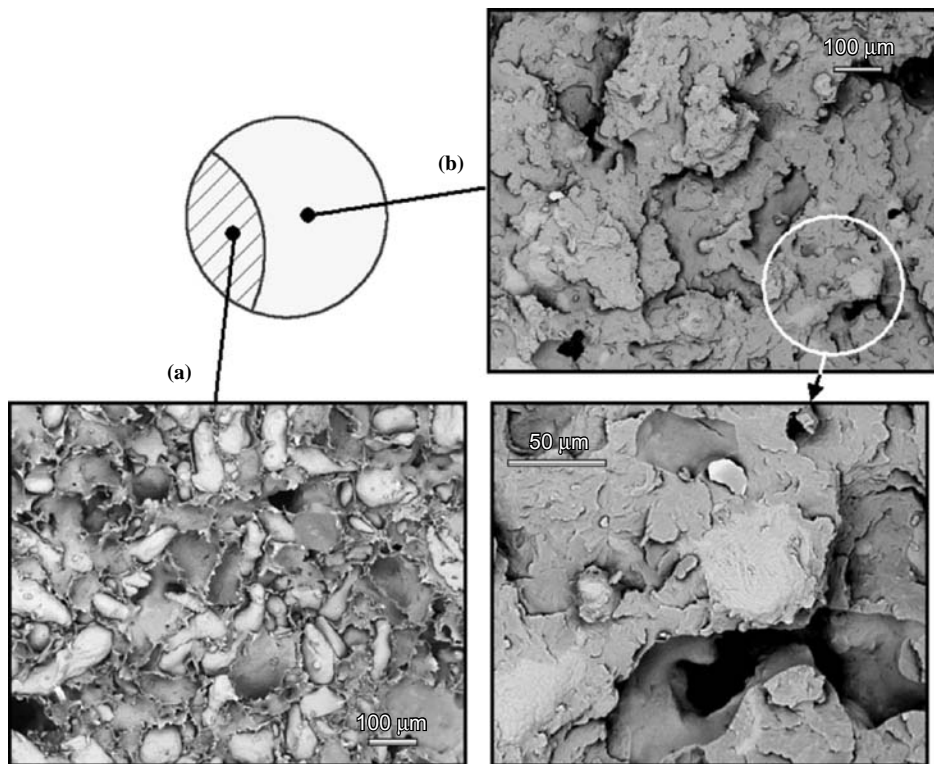

(a)   (b)

Figure 10 Rupture surface typical of PA + Al specimens with the axis // to Z direction

determines the efficacy of the strengthening mechanisms during crack propagation. At a higher level of detail, the combination between a preferential orientation of the filler particles during powder deposition and their sinking in the molten polymer during laser treatment causes a bedding phenomenon. Thus, parts' mechanical response depends on the direction of load application. Both the observed failure mechanisms and the measured mechanical performances are consistent with the model developed.

As a conclusion, the performances of parts produced through AM confirm a strong dependence on the construction geometry and on the powder characteristics. In addition, the present research proves that the initial geometry and deposition modalities of the reinforcing particles are relevant factors too for the considered materials.

References

ASTM D638-08 (2008), *Standard Test Method for Tensile Properties of Plastics*, ASTM, West Conshohocken, PA.

ASTM F2792-09 (2009), *Standard Terminology for Additive Manufacturing*, ASTM, West Conshohocken, PA.

Atzeni, E., Iuliano, L., Minetola, P. and Salmi, A. (2012), "Re-design and cost estimation of rapid manufactured plastic parts", *Rapid Prototyping Journal* (in press).

Atzeni, E., Gatto, A., Iuliano, L., Minetola, P. and Salmi, A. (2009), "A benchmark for accuracy evaluation of dental crowns up-to-date manufacturing", in Jorge Bartolo, P. *et al.* (Eds), *Innovative Developments in Design and Manufacturing*, CRC Press, Boca Raton, FL, pp. 425-30.

Bassoli, E., Gatto, A. and Iuliano, L. (2005), "New developments in steel formulations for direct laser sintering: characterization

and evaluation of joining mechanisms", *Advanced Research in Virtual and Rapid Prototyping*, Taylor & Francis, Rotterdam.

Bassoli, E., Sewell, N.T., Gatto, A. and Johns, D. (2009), "On the effects of building orientation in powder-fed additive layer manufacture of steel 316L", *Innovative Developments in Design and Manufacturing*, Advanced Research in Virtual and Rapid Prototyping, Taylor & Francis, Rotterdam, pp. 263-8.

Bernard, A., Taillandier, G. and Karunakaran, K.P. (2009), "Evolutions of rapid product development with rapid manufacturing: concepts and applications", *International Journal of Rapid Manufacturing*, Vol. 1 No. 1, pp. 3-18.

Berti, G., D'Angelo, L., Gatto, A. and Iuliano, L. (2010), "Mechanical characterisation of PA Al203 composites obtained by selective laser sintering", *Rapid Prototyping Journal*, Vol. 16 No. 2, pp. 124-9.

Bibb, R., Eggbeer, D. and Evans, P. (2010), "Rapid prototyping technologies in soft tissue facial prosthetics: current state of the art", *Rapid Prototyping Journal*, Vol. 16 No. 2, pp. 130-7.

Bugeda, G., Cervera, M. and Lombera, G. (1999), "Numerical prediction of temperature and density distributions in selective laser sintering processes", *Rapid Prototyping Journal*, Vol. 5 No. 1, pp. 21-6.

Caulfield, B., McHugh, P.E. and Lohfeld, S. (2007), "Dependence of mechanical properties of polyamide components on build parameters in the SLS process", *Journal of Materials Processing Technology*, Vol. 182, pp. 477-88.

Dasari, A. and Misra, R.D.K. (2003), "On the strain rate sensitivity of high density polyethylene and polypropylenes", *Mater. Sci. Eng. A*, Vol. 358 Nos 1/2, pp. 356-71.

Eyers, D. and Dotchev, K. (2010), "Technology review for mass customisation using rapid manufacturing", *Assembly Automation*, Vol. 30 No. 1, pp. 39-46.

Giannatsis, J. and Dedoussis, V. (2009), "Additive fabrication technologies applied to medicine and health care: a review", *The International Journal of Advanced Manufacturing Technology*, Vol. 40 No. 1, pp. 116-27.

Gibson, I. and Shi, D. (1997), "Material properties and fabrication parameters in selective laser sintering process", *Rapid Prototyping Journal*, Vol. 3 No. 4, pp. 129-36.

Kruth, J.P., Wang, X., Laoui, T. and Froyen, L. (2003), "Lasers and materials in selective laser sintering", *Assembly Automation*, Vol. 23 No. 4, pp. 357-71.

Masood, S.H. and Song, W.Q. (2004), "Development of new metal/polymer materials for rapid tooling using fused deposition modelling", *Materials and Design*, Vol. 25, pp. 587-94.

Senthilkumaran, K., Pandey, P.M. and Rao, P.V.M. (2009), "Influence of building strategies on the accuracy of parts in selective laser sintering", *Materials and Design*, Vol. 30, pp. 2946-54.

Toni, R., Della Casa, C., Bodria, M., Spaletta, G., Vella, R., Castorina, S., Gatto, A., Teti, G., Falconi, M., Rago, T., Vitti, P. and Sgallari, F. (2009), "A study on the relationship between intraglandular arterial distribution and thyroid lobe shape: implications for biotechnology of a bioartificial thyroid", *Annals of Anatomy – Anatomischer Anzeiger*, Vol. 190 No. 5, pp. 432-41.

Vandenbroucke, B. and Kruth, J.P. (2007), "Selective laser melting of biocompatible metals for rapid manufacturing of medical parts", *Rapid Prototyping Journal*, Vol. 13 No. 4, pp. 196-203.

Violante, M.G., Iuliano, L. and Minetola, P. (2007), "Design and production of fixtures for free-form components using selective laser sintering", *Rapid Prototyping Journal*, Vol. 13 No. 1, pp. 30-7.

Williams, J.D. and Deckard, C.R. (1998), "Advances in modelling the effects of selected parameters on the SLS process", *Rapid Prototyping Journal*, Vol. 4 No. 2, pp. 90-100.

Wohlers, T. (2009), "Rapid prototyping and manufacturing, state of the industry", USA.

Yang, M.Y. and Ryu, S.G. (2001), "Development of a composite suitable for rapid prototype machining", *Journal of Materials Processing Technology*, Vol. 113, pp. 280-4.

Zhang, Y. and Faghri, A. (1999), "Melting of a subcooled mixed powder bed with constant heat flux heating", *International Journal of Heat and Mass Transfer*, Vol. 42, pp. 775-88.

Zhu, H.H., Fuh, J.Y.H. and Lu, L. (2007), "The influence of powder apparent density on the density in direct laser-sintered metallic parts", *International Journal of Machine Tools & Manufacture*, Vol. 47, pp. 294-8.

About the authors

Elena Bassoli has been a Researcher in Technology and Manufacturing Systems at the University of Modena and Reggio Emilia, Italy, since 2005. She received her MS degree in Materials Science Engineering in 2000 and her Doctorate in 2004, discussing a thesis about non-conventional technologies for moulds production. Since, 2008 she has been a member of the scientific Board of CIRTIBS (Interuniversity Research Centre on Innovative Technologies for Instrumentation) in Naples. She is co-author of more than 40 papers and congress communications, regarding innovative technologies. Elena Bassoli is the corresponding author and can be contacted at: elena.bassoli@unimore.it

Andrea Gatto is Full Professor of Technology and Manufacturing Systems at the Faculty of Engineering "Enzo Ferrari" in Modena. He received his MS Degree in Mechanical Engineering in 1988 at Ancona University. His research activity on time compression techniques and non-conventional processes led to the publication of almost 90 papers and congress communications, together with two books. Since, 2008 he has been a member of the scientific Board of CIRTIBS (Interuniversity Research Centre on Innovative Technologies for Instrumentation) in Naples.

Luca Iuliano is a Full Professor Manufacturing Systems at the Department of Production Systems and Business Economics (DISPEA) of the Faculty of Engineering I – Politecnico di Torino, Italy. He received the degree in Electrical Engineering at Politecnico di Torino, Italy in 1985. He is author and co-author of two Italian books on rapid prototyping and investment casting, author and coordinator of a handbook on foundry. He has published over 70 papers in academic journals and in national and international conference proceedings in the following fields: high speed machining (HSM) of nickel based super-alloys and metal matrix composites (MMC); non-conventional machining of nickel-based super-alloys and MMC; reverse engineering (RE); rapid prototyping (RP) and rapid tooling (RT). Luca Iuliano is the president of the Italian Association of Rapid Prototyping (APRI).